Mode of lithospheric extension: Conceptual models from analogue modeling

Laurent Michon, Olivier Merle

Mode of lithospheric extension: Conceptual models from analogue modeling

Laurent Michon[1]

Netherlands Organization for Applied Scientific Research–Netherlands Institute of Applied Geoscience (TNO-NITG), Utrecht, Netherlands

Olivier Merle[2]

Laboratoire Magmas et Volcans, Université de Clermont, Clermont-Ferrand, France

[1] Comparison of analogue experiments at crustal and lithospheric scale provides essential information concerning the mode of deformation during lithospheric extension. This study shows that during extension, lithospheric deformation is controlled by the development of shear zones in the ductile parts. At lithospheric scale, the global deformation is initiated by the rupture of the brittle mantle lithosphere. This failure generates the formation of conjugate and opposite shear zones in the lower crust and the ductile mantle lithosphere. The analysis of the internal strain of the ductile layers suggests that the two opposite shear zones located below the asymmetric graben in the lower crust and the ductile mantle lithosphere prevail. Experiments show that from a similar initial stage, the relative predominance of these shear zones originates two different modes of deformation. If the crustal shear zone prevails, a major detachment-like structure crosscuts the whole lithosphere and controls its thinning. In this model named the simple shear mode, the resulting geometry shows that crustal and lithospheric thinning are laterally shifted. If the mantle shear zone predominates, the lithospheric thinning is induced by the coeval activity of the two main shear zones. This process called the necking mode leads to the vertical superposition of crustal and mantle lithospheric thinning. Applied to natural laboratories (West European rift, Red Sea rift and North Atlantic), this conceptual model allows a plausible explanation of the different geometries and evolutions described in these provinces. The North Atlantic and the Red Sea rift systems may result from a simple shear mode, whereas the necking mode may explain part of the evolution of the West European rift especially in the Massif Central and the Eger graben.   INDEX TERMS: 8109 Tectonophysics: Continental tectonics—extensional (0905); 1744 History of Geophysics: Tectonophysics; 1645 Global Change: Solid Earth; 9335 Information Related to Geographic Region: Europe; *KEYWORDS:* lithospheric extension, analogue modeling, West European rift, Red Sea rift, passive margins. **Citation:** Michon, L., and O. Merle, Mode of lithospheric extension: Conceptual models from analogue modeling, *Tectonics*, *22*(4), 1028, doi:10.1029/2002TC001435, 2003.

1. Introduction

[2] The asymmetric feature of continental rifts has been clearly demonstrated during the past decades, whatever the origin of rifting (i.e., passive or active rifting) [e.g., *Mart and Hall*, 1984; *Bosworth*, 1985; *Brun et al.*, 1992; *Rosendahl et al.*, 1992]. Although a single passive margin presents an asymmetric geometry, conjugate and opposite margins like in the northern Atlantic (the Canadian and Iberian margins) mostly reveal a symmetric shape at the lithospheric scale [*Lister et al.*, 1991; *Brun and Beslier*, 1996]. Contrary to *McKenzie* [1978] and *Wernicke* [1981, 1985], who have respectively advocated pure shear and simple shear to interpret lithospheric deformations, *Cochran and Martinez* [1988], *Lister et al.* [1991] and *Kusznir and Ziegler* [1992] have assumed a combination of both simple and pure shear to explain these different geometries. According to these authors, crustal deformation may be controlled by low angle detachment faulting, and thinning of the mantle lithosphere may result from pure shear. Such models have been improved by *Beslier* [1991] and *Brun and Beslier* [1996] to explain the occurrence of shear zones in the mantle lithosphere [*Girardeau et al.*, 1988; *Vissers et al.*, 1995]. These authors have proposed that mantle lithospheric thinning could result from a necking of the lithosphere, generated by opposite and conjugate shear zones (Figure 5 of *Brun and Beslier* [1996]).

[3] In the present paper, we first summarize the main characteristics of several continental rifts and passive margins in order to show the different geometries resulting from extension. We have selected a number of structures which formed in different geodynamical contexts during the Mesozoic or the Cenozoic: the West European rift, the

---
[1]Also at Geologisches Institut, Universität Freiburg, Freiburg, Germany.
[2]Now at Laboratoire Magmas et Volcans, OPGC, Université Blaise Pascal, CNRS, Clermont-Ferrand, France.
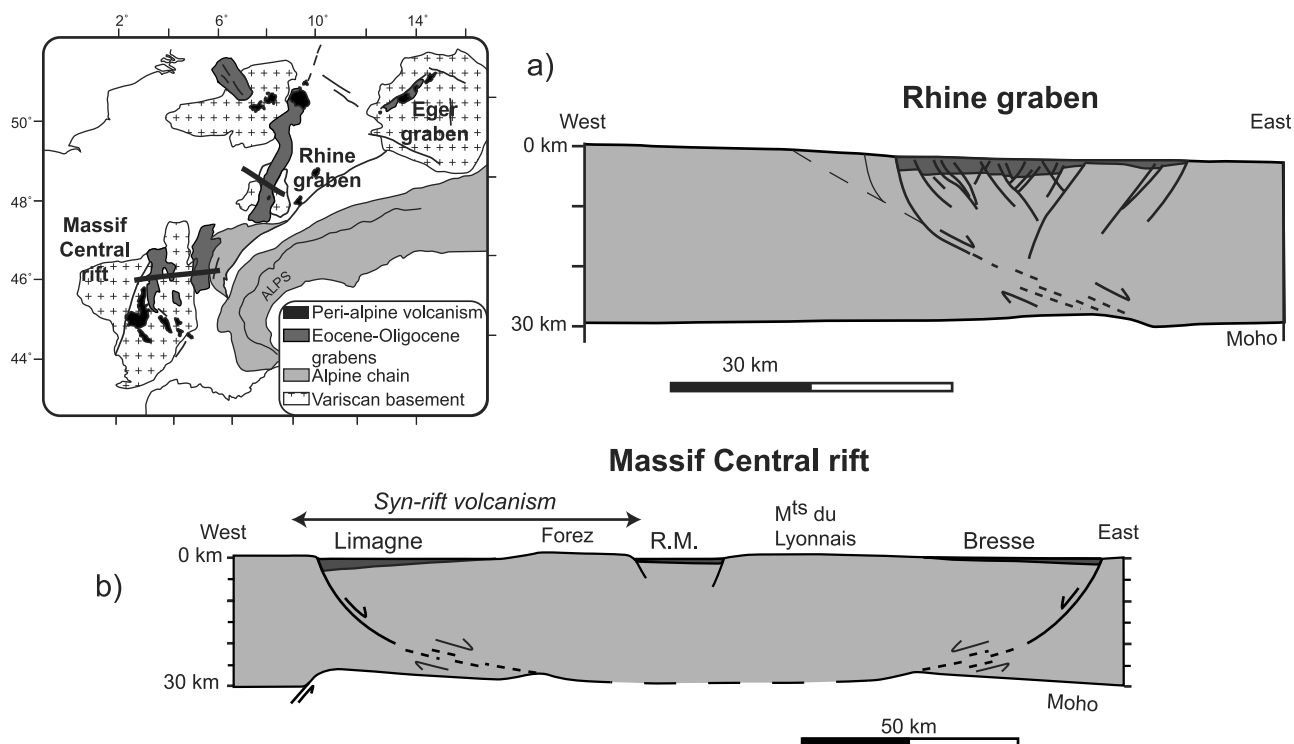
Figure 1. Synthetic geological map of the West European rift showing the Massif Central rift, the Rhine graben and the Eger graben. (a) Crustal cross section of the southern part of the Rhine graben showing the asymmetry of the graben (modified after *Brun et al.* [1992]). The master fault bounds the graben in the west and is probably connected to the Moho by a shear zone in the lower crust. (b) Crustal geometry of the Massif Central rift. The mirror symmetry revealed by the graben geometry and the Moho inflexions below the Forez and the Monts du Lyonnais results from symmetric extension between Priabonian and middle Oligocene. The development of the syn-rift volcanism in the western part of the rift and the Moho inflexion below the Limagne master fault are interpreted as the consequence of an asymmetric extension during upper Oligocene and lower Miocene.

North Atlantic passive margins and the Red Sea rift. According to the age of the continental lithosphere in each province, we assume that the vertical strength profile corresponds to a 4-layer model with two brittle high strength levels (the upper crust and the upper mantle lithosphere) and two ductile layers (the lower crust and the lower mantle lithosphere). In such a context, it has been suggested that the lithospheric deformation is initiated and controlled by failure of the brittle mantle lithosphere [*Brun and Beslier*, 1996].

[4] As the aim of this paper is to determine the process leading to continental rifts at lithospheric scale, we compare scaled analogue experiments at crustal scale [*Michon and Merle*, 2000] and lithospheric scale [*Brun and Beslier*, 1996]. In the 4-layer model, which represents the lithospheric strength profile, strain analysis of the ductile layers makes possible to define two main shear zones, which control the deformation and the thinning of the models after the boudinage of the brittle mantle lithosphere. This study shows that the simple shear mode and the necking of the lithosphere result from a similar initial evolution. Finally, we propose a model that can explain the various evolutions and geometries observed in the

West European rift, the North Atlantic passive margin and the Red Sea rift.

2. Natural Laboratories

2.1. West European Rift

[5] The West European rift is composed of three provinces extending from the Bohemian Massif in the east, through the Rhenish Province in the central part, to the Massif Central in the west (Figure 1). In all provinces, extension started contemporaneously 40 m.y. ago and led to the formation of a set of grabens and a syn-rift volcanic activity [*Michon*, 2001]. The global evolution with extension and sedimentation near sea level, closely followed in the Massif Central and the Eger graben (Bohemian Massif) by a volcanic activity, is interpreted in terms of passive rifting evolution [*Bois*, 1993; *Merle et al.*, 1998].

[6] In the Rhenish Province, the Rhine graben is a linear structure which results from W/WNW-E/ESE extension. Geophysical data clearly show that the Rhine graben is a single asymmetric graben of 35–40 km wide, which is associated with strong crustal thinning [*Brun et al.*, 1992].

In the north, the half graben is bounded in the east by a west dipping major fault. South to the Lalaye-Lubine-Baden-Baden Variscan fault, the asymmetry is reversed and the graben is limited in the west by an east dipping master fault (Figure 1a). The distribution of the depocenters close to these master faults reveals that the faults have controlled the subsidence [*Doebl and Olbrecht*, 1974; *Villemin et al.*, 1986]. From the Priabonian to the end of the middle Oligocene, a similar subsidence rate [*Villemin et al.*, 1986] and sedimentation at sea level [*Sissingh*, 1998] characterize the northern and southern parts suggesting that the amount of extension was identical at the graben scale. From the Late Oligocene, subsidence drastically decreased in the southern part whereas it was ongoing in the northern segment up to Middle Miocene. After an interruption of sedimentation during the Late Miocene, the northern Rhine graben was reactivated at the beginning of the Pliocene [*Sissingh*, 1998]. Subsidence was still active in the Pleistocene in the northern part and restarted in the southern part [*Schumacher*, 2002]. Whereas the Eocene-Oligocene rifting is clearly related to the extension of the West European rift, this latter extensional episode is closely associated with the recent evolution of the Roer Valley graben and the southern North Sea [*Kooi et al.*, 1991; *Zijerveld et al.*, 1992]. The twofold evolution of the northern part of the Rhine graben has resulted in a thicker pile of sediments and stronger crustal thinning than in the southern part. In the northern part of the Rhine graben, the stretching value deduced from the geometry of the faults in the upper crust is estimated to be in the range from 5 to 7 km. Assuming preservation of the volume of the crust, a total extension value of about 17 km can be deduced [*Brun et al.*, 1992]. In the southern part, the extension value estimated from preservation of the volume of the crust is about 12 km [*Bois*, 1993]. As it has been shown that the northern segment was affected by two distinct periods of extension, the extension value resulting from the West European rift episode only is probably about 12 km. Thus the extension rate deduced from the 10 m.y. Priabonian-Middle Oligocene rifting episode is close to 1.2 mm/yr.

[7] The Massif Central rift, which is the most important segment of the West European rift, has been recently reinterpreted [*Merle et al.*, 1998; *Michon*, 2001]. The Variscan basement is affected by a north-south 180 km wide rift composed by Eo-Oligocene grabens. Along an east-west cross section, the rift is characterized by two lateral and opposite half grabens (the Limagne graben in the west and the Bresse graben in the east) and a central and near-symmetric graben (the Roanne-Montbrison graben) (Figure 1b). Geophysical data show that the structure is bounded by the two opposite detachment faults of the Limagne and Bresse half grabens which might be connected at depth to the Moho discontinuity [*Michon*, 2001]. This overall geometry reveals a strikingly mirror symmetry on both sides of the central part of the Roanne-Montbrison graben (Figure 1b). The east-west cross section also shows asymmetrical features at the scale of the rift. The Moho inflexion below the Limagne half graben and the occurrence of a magmatic activity restricted in the western

part of the rift correspond to geological characteristics which are hardly compatible with a purely symmetric evolution. The explanation can be found in the sedimentary record [*Merle et al.*, 1998]. Similar deposits in the Limagne and Bresse half grabens from the Late Eocene to the Early Oligocene together with sedimentation at sea level [*Giraud*, 1902; *Rat*, 1974; *Bodergat et al.*, 1999] suggest a symmetric extension during this period. However, in the Late Oligocene, persistence of marine incursions in the Limagne half graben and the lack of marine incursion and the lull in sediment deposits in the Bresse graben show that the overall symmetrical evolution came to a halt. During this period, crustal thinning occurred in the western Limagne graben. This is clearly established from geophysical profiles where crustal thinning reaches 25% in the Limagne graben whereas it does not exceed 13% in the Bresse graben. The asymmetric extension during the Late Oligocene is confirmed by the occurrence of a scattered magmatic activity in the Limagne half graben. Then, we interpret the mirror symmetry as resulting from the Late Eocene-Middle Oligocene symmetric extension whereas the Late Oligocene-Early Miocene evolution corresponds to an asymmetric extension located in the western part of the rift only. The stretching value deduced from master fault geometries in the upper crust is inferior to 10–15 km. However, as in the Rhine graben, this value is more than two times lower than the value estimated from geophysical data, which is close to 25–30 km [*Bois*, 1993]. Again, this discrepancy may be explained by ductile flow in the lower crust. The extension rate estimated for the Massif Central rift ranges from 2.5 to 3 mm/yr.

[8] In the Bohemian Massif, the evolution and the geometry of the Eger graben are still poorly constrained. This graben is 40–45 km wide, trending N60°E, and is bounded in the north by a main normal fault (the Krušné Hory fault), which gives to the whole structure a global asymmetry. The Priabonian age of the oldest sediments related to the extension [*Chlupac et al.*, 1984] indicates that the graben formation was coeval with the formation of the Massif Central rift and the Rhine graben. The thickness of the Late Oligocene-Middle Miocene sediments never exceeds 500–600 m and the depocenter are located close to the Krušné Hory fault suggesting (1) a small amount of extension and (2) a major role of this master fault in the graben evolution. From the Middle Oligocene (i.e., 10 m.y. ago after the onset of the extension) and up to the Middle Miocene, a syn-rift volcanic activity was located within the graben leading to the formation of large magmatic provinces [*Ulrych et al.*, 2000]. Despite the few amount of data, the formation of a single asymmetric graben and the development of a syn-rift volcanic phase within the extensional area correspond to geological information of primary importance, which can be help to determine the evolution and the deformation of the whole lithosphere.

2.2. North Atlantic Passive Margins

[9] The understanding of the North Atlantic passive margins has been largely improved by the discovery of a
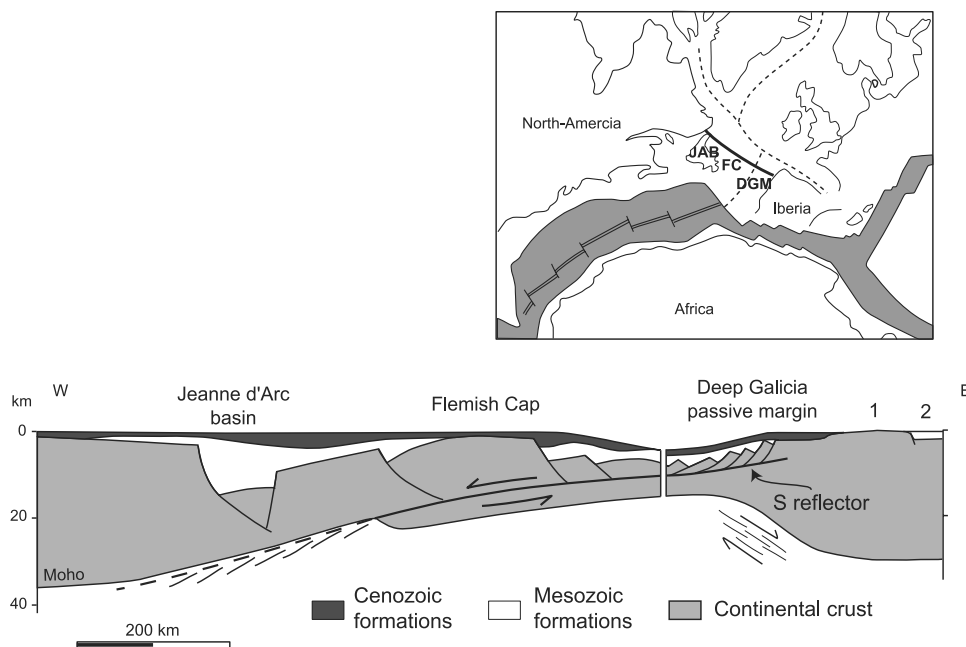
Figure 2. Reconstruction of the North Atlantic passive margin before oceanization (after *Tankard and Welsink* [1987]). In this cross section, only structures resulting from the main period of extension are represented (see text for explanation). 1: Galicia bank. 2: Interior Basin. JAB: Jeanne d'Arc Basin. FC: Flemish Cap. DGM: Deep Galicia Margin.

mantle ridge close to the ocean-continent transition zone in the Galicia passive margin [*Boillot et al.*, 1980]. At the latitude of Iberia, geophysical and tectonic studies have allowed to reconstruct the initial geometry of the rift before oceanization taking into account both Galicia and East Canadian margins (Figure 2) [*Tankard and Welsink*, 1987]. Seismic data show that the East Canadian margin is composed from west to east of a nearly symmetric graben (the Jeanne d'Arc basin) and a horst (the Flemish cap). The subsidence analysis of the Jeanne d'Arc basin reveals a main period of quick subsidence during the Late Barremian (around 120 Ma) [*Driscoll et al.*, 1995]. In the east, the Iberian margin can be divided in two different parts: the Interior Basins (Interior and Porto basins) and the Deep Galicia margin. The Interior Basins correspond to symmetric grabens of the proximal part of the margin which were active from the very beginning of the extension (i.e., Valanginian) [*Manatschal and Bernoulli*, 1999]. In contrast, the Deep Galicia margin is composed of eastward tilted blocks which yield a strongly asymmetric structure. The age of the syn-rift sediments (Hauterivian to Aptian) suggests that the extension has shifted from the Interior Basins to the Deep Galicia margin during rifting [*Manatschal and Bernoulli*, 1999]. Stretching values have been deduced for the whole period of rifting (300–350 km) [*Keen and Dehler*, 1993]. However, the multiphase extension in the North Atlantic leading to continental breakup as well as the previous extension in the Interior Basin [*Manatschal and Bernoulli*, 1999] make it difficult the estimation of the stretching value related to the main phase of rifting (Hauterivian to Albian).

[10] One of the main characteristics of the Galicia passive margin is the presence of a prominent seismic reflector, the so-called S reflector. In the Deep Galicia margin, the S reflector is located at the base of the tilted blocks and its dip evoluates from westward dipping in the east to a slightly eastward dipping close to the mantle ridge [*Boillot et al.*, 1980, 1988; *Mauffret and Montadert*, 1987]. In this area, the S reflector directly overlies the mantle ridge and seems to have merged into seafloor. Whereas the S reflector is mainly interpreted as a top-to-the-ocean low-angle detachment structure which was responsible for mantle exhumation during rifting [e.g., *Beslier et al.*, 1990; *Reston et al.*, 1996; *Manatschal and Bernoulli*, 1999], the origin and the age of a second opposite shear zone (top-to-the-continent) in the mantle peridotite is still a matter of controversy. *Boillot et al.* [1995] and *Brun and Beslier* [1996] have proposed to explain the mantle exhumation by the development of two nearly synchronous and opposite shear zones in both the lower crust and the mantle lithosphere leading to the necking of the lithosphere. According to this model, the S reflector and the mantle shear zone could correspond to the detachment structures in the lower crust and the mantle, respectively. However, using $^{40}Ar/^{39}Ar$ ages [*Féraud et al.*, 1988], *Manatschal and Bernoulli* [1999] have shown that the tectonic activity of the mantle shear zone is slightly older than the crustal one and have proposed that both mantle and crustal structures result from two different stages in continental extension. Whatever the exact chronology of these two detachment faults, the evolution of the syn-rift subsidence in both East Canadian and Galicia
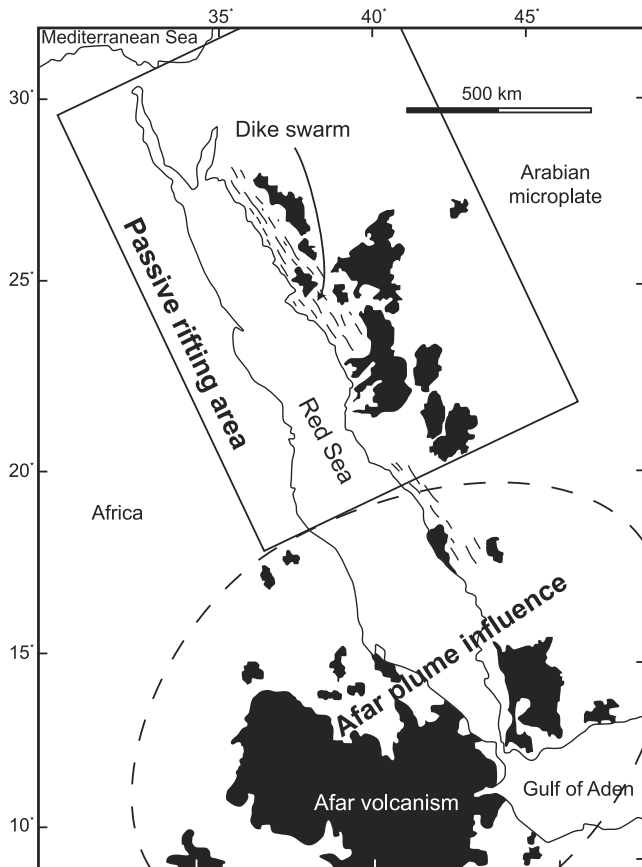
Figure 3. Geological map of the Red Sea area showing the distribution of the syn-rift volcanism on the Arabian microplate only.

opposite margins suggests that (1) maximal crustal thinning was superimposed on the two graben areas (Jeanne d'Arc basin and Deep Galicia margin) and that (2) mantle lithospheric thinning took place in the eastern part of the rift (i.e., east to the Flemish Cap) (Figure 12 of *Keen and Dehler* [1993]).

2.3. Red Sea Rift

[11] The Red Sea rift is a 1700 km length NNW-SSE oriented narrow rift which is located north to the Afar area (Figure 3). During the last decades, this rift was the subject of two main controversies. On one hand, the debate focuses on the origin of the extension (i.e., passive rifting versus active rifting) and the relation with the Afar plume [*Courtillot*, 1980; *Dixon et al.*, 1989; *Bohannon et al.*, 1989]. Recently, *Menzies et al.* [1997] have proposed that the extension in the northern Red Sea results from the northward propagation of the southern Red Sea, which is linked to the Afar plume. In their model, an active rifting origin is clearly advocated for the southern Red Sea, whereas the evolution of the northern segment can be interpreted in terms of passive rifting. On the other hand, assuming that the Red Sea rift results from a passive

rifting evolution, two opposite modes of extension have been proposed to explain the main geological and geophysical features of the area. *Wernicke* [1985] has referred to the development of a low-angle detachment structure (i.e., simple shear mode) to induce volcanism and uplift in the eastern border of the rift only (in the Saudi Arabian microplate). In contrast, *Buck et al.* [1988] have advocated a pure shear mode with an initial 110 km wide rifting area becoming narrower with time (20 km wide) to explain the present-day high and narrow heat flow in the central Red Sea. It is well worth noting that the simple shear mode is based on Eo-Miocene geological features, whereas present-day data are used to define the pure shear model. Consequently, these two modes of extension are deduced from different periods: the simple shear mode for an initial continental extension and the pure shear mode for a nearly oceanization stage.

[12] As the southern part of the Red Sea rift presents strong interactions with the Afar plume, we will summarize the main Oligo-Miocene geological features of the northern Red Sea in order to constrain the evolution of the rifting. Although the onset of the extension is not well established, *Bohanonn et al.* [1989] have suggested a normal faulting activity with sedimentation close to sea level from 23 to 29 Ma, with an increased extension rate around 25 Ma. During this period a first phase of volcanism started in the Arabian margin only. The age of the onset of magmatism is poorly constrained. K/Ar ages mainly obtained in the 1970s and 1980s suggest the occurrence of volcanism around 30–32 Ma (i.e., before extension) [*Brown et al.*, 1984]. However, several combined K/Ar and $^{40}Ar/^{39}Ar$ data have often shown strikingly differences between ages obtained with both methods suggesting that ages based on the K/Ar method must be handled with care [*Baker et al.*, 1996; *Rittmann and Lippolt*, 1998]. The oldest lava flows dated from the $^{40}Ar/^{39}Ar$ method in Saudi Arabia indicate an onset of the volcanic activity coeval with the beginning of the extension (27–28 Ma) [*Chazot et al.*, 1998]. After a lull of volcanism during several millions years, the Arabian margin was again affected by an intense magmatic phase coeval with a main period of continental rifting between 21–24 Ma [*Chazot et al.*, 1998]. This magmatism led to the formation of a 1000 km length dyke swarm parallel to the newly formed continental rift. Finally, from the Early Miocene (ca. 20 Ma), the Arabian margin was uplifted causing the present-day topographic asymmetry on either side of the Red Sea [*Bohannon et al.*, 1989]. According to many authors [e.g., *Wernicke*, 1985; *Bohannon et al.*, 1989], we consider that this general evolution of the period of continental rifting (i.e., rifting at sea level, volcanism and uplift) can be interpreted in terms of passive rifting. The overall geometry resulting from this Oligo-Miocene event reveals a strong asymmetry of the spatial distribution of magmatism and uplift restricted to the Arabian microplate. Likewise, this asymmetry can be readily seen in the seafloor topography of the Northern Red Sea (Figure 5 of *Cochran and Martinez* [1988]). The bathymetry decreases abruptly between the western shore
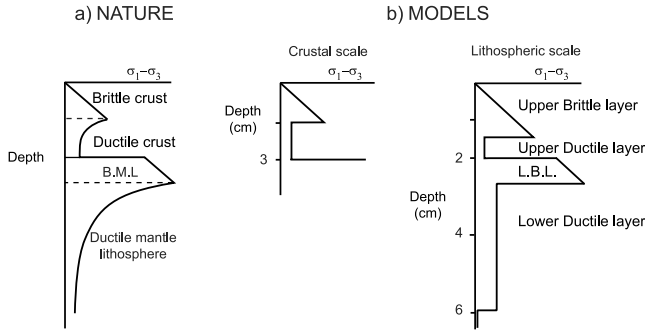
Figure 4. Strength profile (a) for a continental lithosphere with a normal thermal gradient and (b) in experiments. Sand is used to simulate the brittle parts of the lithosphere and silicone putty mimics the behavior of the lower crust and the ductile mantle lithosphere.

and the central axis of the Red Sea, whereas it gradually increases from the axial zone up to the eastern border. Contrary to the Oligo-Miocene asymmetric features, the present-day heat flow and seismicity distribution reveals a symmetric geometry [*Cochran and Martinez*, 1988; *Dixon et al.*, 1989], which could indicate a change in the rifting evolution.

[13] Although the extension rate of the northern Red Sea is fairly well estimated from the Late Miocene to the present-day (1cm/yr) [*Cochran and Martinez*, 1988], the stretching values and the extension rate are not known for the pre-Late Miocene period. Assuming that most of the extension has occurred in the past 12–14 Ma [*Le Pichon and Gaulier*, 1988], the extension rate may have been very slow during the initial period of rifting.

3. Analogue Experiments of Continental Extension

[14] In this part, we compare analogue experiments already published and carried out at crustal [*Michon and Merle*, 2000] and lithospheric scale [*Brun and Beslier*, 1996]. These experiments resulting from independent studies, we first develop a common scaling approach defining several dimensionless numbers for the crustal and lithospheric experiments, in order to show that these experiments are properly scaled.

3.1. Experimental Background

[15] The analogue models can be compared to the natural systems if the distribution of stresses, densities and rheologies are similar in nature and experiments [*Hubbert*, 1937]. In the areas presented in the first sections of this paper, the lithosphere is assumed to have a normal thermal gradient before the rifting event. It is generally accepted [e.g., *Ranalli and Murphy*, 1987; *Buck*, 1991; *Davy and Cobbold*, 1991; *Fernandez and Ranalli*, 1997; *Burov and Poliakov*, 2001] that with such a thermal gradient (Moho-temperature less than 500°–600°C), the strength profile of the lithosphere before the rifting process is characterized from top to bottom by a brittle upper crust, a ductile lower crust, a brittle mantle lithosphere and a ductile mantle lithosphere (Figure 4a). The rheological structure of the lithosphere being highly dependent on the thermal gradient and the strain rate, this theoretical 4-layer strength profile can change during the thinning of the lithosphere with a shift of the brittle-ductile transition in the crust and the mantle lithosphere [*Davy and Cobbold*, 1991]. Experiments at lithospheric scale have been carried out with a 4-layer brittle-ductile model whereas experiments at crustal scale correspond to the upper part of the strength profile only (Figure 4b). In both experiments, the ductile and brittle behaviors of the lithosphere were simulated by silicone putty and sand layers, respectively. Although the behavior of the lithospheric ductile levels is characterized by a power law rheology, *Davy and Cobbold* [1991] have shown that the use of the silicone putty is a good approximation to simulate the lithospheric ductile parts.

[16] Numerical approaches show that the thermal regime of the lithosphere could play a major role on the mode of deformation during a rifting event [e.g., *Buck*, 1991; *Burov and Poliakov*, 2001]. The influence of the temperature

Table 1. Geometric and Mechanical Variables in Nature and Experiments at Crustal and Lithospheric Scale

Variable	Definition	Nature	Experiments		Dimensions
			Crustal Scale	Lithospheric Scale	
h_{UBL}	thickness of the upper crust (UBL)	$15-18 \times 10^3$	1.5×10^{-2}	$1.2-1.4 \times 10^{-2}$	m
h_{UDL}	thickness of the lower crust (UDL)	$12-15 \times 10^3$	1.5×10^{-2}	$0.5-0.6 \times 10^{-2}$	m
H_c	thickness of the crust (UBL + UDL)	$30-35 \times 10^3$	3×10^{-2}	$1.7-2 \times 10^{-2}$	m
H_{ML}	thickness of the mantle lithosphere (LBL + LDL)	$70-90 \times 10^3$	-	$2.3-2.8 \times 10^{-2}$	m
ρ_{UBL}	density of the upper crust (UBL)	2700	1400	1400	kg/m^3
ρ_{UDL}	density of the lower crust (UDL)	2800	1350	1100–1214	kg/m^3
ρ_{LBL}	density of the brittle mantle lithosphere (LBL)	3300	-	1400	kg/m^3
ρ_{LDL}	density of the ductile mantle lithosphere (LDL)	3300	-	1305	kg/m^3
Φ	angle of internal friction	30°	30°	30°	
μ	viscosity	1×10^{21}	3×10^4	$1.3-2.1 \times 10^4$	Pa.s
$\tau 0$	cohesion	2×10^6	1	1	Pa
ε	strain rate	5×10^{-15}	1.8×10^{-4}	$2.3 \times 10^{-4} - 2.3 \times 10^{-3}$	s^{-1}
g	gravity acceleration	10	10	10	m/s^2

Table 2. Π Dimensionless Numbers in Nature and Experiments

Dimensionless Parameter	Definition	Nature	Experiments	
			Crustal Scale	Lithospheric Scale
Π_1	UBL/UDL thickness	$1-1.5$	1	$2.3-3$
Π_{1b}	crust/mantle lithosphere thickness	0.4	-	$0.6-0.85$
Π_2	angle of internal friction	30	30	30
Π_3	UBL/UDL density	0.96	1.04	$1.12-1.27$
Π_{3b}	LBL/LDL density	1	-	1.07
Π_4	gravitational/viscous stresses	81	37.5	$4-34.5$
Π_5	inertial/viscous stresses	3×10^{-24}	2.9×10^{-11}	$5.6 \times 10^{-9}-1.57 \times 10^{-11}$
Π_6	failure resistance/viscous stresses	31.75	15.16	$2.1-16.08$
Π_7	gravitational stress/cohesion	202.5	210	$168-196$

cannot be included directly in the analogue experiments. Nevertheless, in the experiments, a change of the thickness ratio between the brittle and ductile layers (i.e., thick upper crust and thin lower crust or thin upper crust and thick lower crust) is able to simulate different initial geotherms from an old and cold lithosphere up to a young and hot lithosphere. In addition, *Michon and Merle* [2000] have shown that the initial thermal regime of the lithosphere is a parameter that has a minor influence on the crustal deformation. Then, we consider that for the study of the first stage of a rifting process, analogue approach can be used to study the mode of deformation of the lithosphere.

[17] To guarantee similarity in nature and experiments, we define several variables related to the geometry and the properties of the materials (Table 1). The geometry of the different parts of the lithosphere is characterized by the thickness of the Upper Brittle Layer h_{UBL} (i.e., the upper crust in nature), the Upper Ductile Layer h_{UDL} (i.e., the lower crust), the whole crust H_C and the mantle lithosphere H_{ML}. Materials property variables are the density of the Upper Brittle Layer ρ_{UBL}, of the Upper Ductile Layer ρ_{UDL}, of the Lower Brittle Layer ρ_{LBL} and of the Lower Ductile Layer ρ_{LDL}. The viscosity μ of the ductile layer, and the internal angle of friction Φ and the cohesion τ_o of the brittle levels are also variables related to the materials properties. The relation between the deformation and the time corresponds to the strain rate ε. Finally, the only force is the gravity acceleration g.

[18] According to the Buckingham-Π theorem, there are 10 variables minus 3 dimensions equal to 7 independent dimensionless numbers (Table 2) that need to maintain the same value in nature and experiments. Of these, two dimensionless parameters correspond to the geometric ratios of the system:

$$\Pi_1 = \frac{h_{UBL}}{h_{UDL}}, \tag{1}$$

$$\Pi_{1b} = \frac{H_C}{H_{ML}}. \tag{2}$$

[19] In equation (1), h_{UBL} and h_{UDL} represent the thickness of the Upper Brittle Layer UBL (i.e., the brittle upper crust in nature) and the Upper Ductile Layer UDL of the system (i.e., the ductile lower crust), respectively. The second dimensionless parameter Π_{1b} is only used to scale the lithospheric experiments and corresponds to the thickness ratio between the crustal H_C and mantle lithospheric H_{ML} levels.

[20] The third dimensionless number can be defined as the frictional angle of the brittle material:

$$\Pi_2 = \Phi. \tag{3}$$

Two other dimensionless parameters must be related to the density ratio of the different layers.

$$\Pi_3 = \frac{\rho_{UBL}}{\rho_{UDL}}, \tag{4}$$

$$\Pi_{3b} = \frac{\rho_{LBL}}{\rho_{LDL}}. \tag{5}$$

[21] Π_3 defines the density ratio between the UBL and the UDL, whereas Π_{3b} allows to scale the density of the Lower Brittle Layers LBL and Lower Ductile Layers LDL in the experiments at lithospheric scale only.

[22] Knowing that gravity is balanced in the brittle materials by stresses that resist failure and in the ductile levels by inertial and viscous stresses, we define three other dimensionless parameters, which correspond to ratios of these stresses:
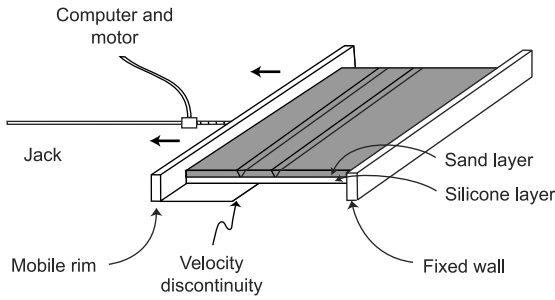
$$\Pi_4 = \frac{\rho g h_{UBL}}{\varepsilon \mu}, \tag{6}$$

$$\Pi_5 = \frac{\varepsilon \rho h_{UBL}^2}{\mu}, \tag{7}$$

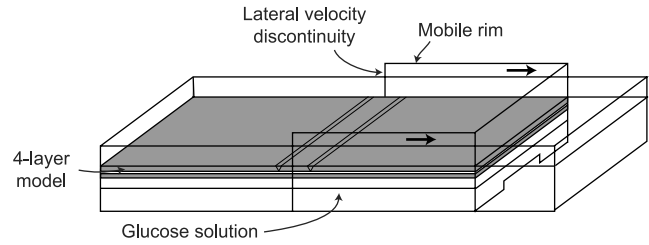$$\Pi_6 = \frac{2 \tan \Phi \rho g h_{UBL}}{3 \varepsilon \mu} + \tan \Phi. \tag{8}$$

[23] Equations (6), (7) and (8) represent respectively ratios between the gravitational stress and the viscous stress, the inertial stress and the viscous stress (i.e., the Reynolds

a-

b-

Figure 5. Experimental setup used in analogue experiments at (a) crustal and (b) lithospheric scale. Apparatus at lithospheric scale after *Brun and Beslier* [1996].

number) and the failure resistance stress and the viscous stress (see *Merle and Borgia* [1996] for details).

[24] Finally, the last dimensionless parameter corresponds to the ratio of gravitational stress to cohesion:

$$\prod_7 = \frac{\rho g h_{\text{UBL}}}{\tau_0} \qquad (9)$$

Results of equations (1), (1b), (3) and (3b) clearly show the similarity between nature and the experiments at both scales for the geometry and the density of the materials (Table 2). The angle of internal friction is the same for the sand and natural rocks (30°). Considering an average strain rate in nature (5×10^{-15} s^{-1}) and a viscosity of the lower crust of $\sim\mu = 10^{21}$ Pa s, Π_4 and Π_6 impose a strain rate in the experiments around 10^{-4}–10^{-3} s^{-1}. The very small value of Π_5 in nature (3.1×10^{-24}) shows that the inertial forces are negligible with respect to the viscous forces. In the experiments, such a low value cannot be reached even using materials with high viscosity and low density. Nevertheless, in experiments the low values of Π_5 (5.6×10^{-9}–1.57×10^{-11}) suggest that the inertial forces have also a minor importance with respect to the viscous forces. Thus this number may receive no further consideration. The last dimensionless parameter Π_7 is partly derived from the cohesion of the materials. The cohesion of intact and massive rock is considered to be $\sim10^7$ Pa [*Jaeger and Cook*, 1971]. However, it is widely accepted that the cohesion could decrease of 1 or 2 orders of magnitude for fractured rocks [e.g., *Merle et al.*, 2001]. In nature, the continental crust is generally affected by numerous faults resulting from different tectonic events (e.g. the Variscan continental crust in Europe). Then, it is reasonable to consider that the cohesion of the crust at a large scale is closer to 10^6 Pa than 10^7 Pa (Table 1). The resulting Π_7 is similar in nature and in experiments at crustal and lithospheric scale (Table 2).

[25] This scaling approach finally shows that (1) experiments carried out by independent studies [*Beslier*, 1991; *Brun*, 1999; *Michon and Merle*, 2000] can be compared and (2) the results and interpretation can be applied to natural laboratories.

[26] It has been proposed that the deformation in a lithosphere is initiated by failure in the brittle mantle lithosphere [*Allemand et al.*, 1989; *Brun and Beslier*, 1996]. In numerical modeling, such a failure is usually simulated by a preexisting weak zone in the lithosphere [e.g., *Huismans and Beaumont*, 2002]. In the analogue experiments, the rupture in the brittle mantle lithosphere was initiated by a velocity discontinuity (VD), which was forced by the border of a moving plastic sheet (Figure 5). As in the numerical approach, the VD concentrates the deformation and controls the development of the structures. At crustal scale, the VD was located at the base of the system (i.e., below the silicone layer corresponding to the lower crust), whereas it was situated on the vertical lateral boundaries of the apparatus in the experiments at lithospheric scale (Figure 5). Contrary to the analogue modeling at lithospheric scale, *Michon and Merle* [2000] have carried out experiments with one but also two VDs in order to determine the role of the number of ruptures upon crustal deformation. In experiments with one VD, the use of a vertically stratified silicone has allowed the analysis of the internal strain within the ductile layers and the determination of the highest strain zones (i.e., the shear zones).

3.2. Summary of Previous Studies

[27] Analogue experiments of continental rifting have been conducted during the last decade at crustal [*Michon and Merle*, 2000] and lithospheric scale [*Beslier*, 1991; *Brun and Beslier*, 1996; *Chemenda et al.*, 2002]. These studies have shown that major parameters control the mode of deformation and the strain during a rifting process: the extension rate and the development of shear zone in the mantle lithosphere and the crust. We summarize herein the main observations.

[28] Experiments with one VD and various extension rates show in both studies the occurrence of two deformation styles distinguished by the number of grabens. Low extension rate leads to the formation of a single half-graben on the movable part (Figure 6a). At both crustal and lithospheric scales, this asymmetric graben is bounded by a master fault in the brittle upper part, which is rooted along a slight silicone upwelling. In contrast, high extension rate

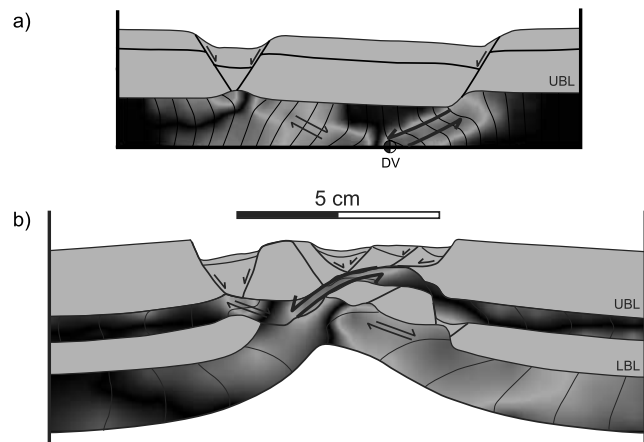a) **Low extension rate**   b) **High extension rate**
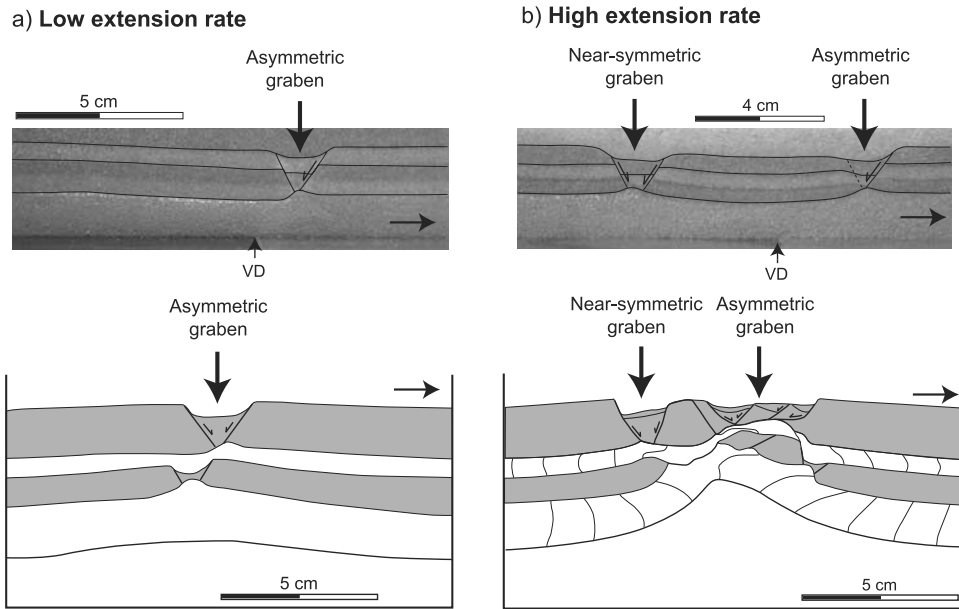
Figure 6. Comparison between experiments carried out at crustal and lithospheric scale. (a) At low extension rate the extension induces the formation of a single asymmetric graben on the movable part. (b) In contrast, a high extension rate leads to the creation of two grabens: a near-symmetric graben in the motionless part and an asymmetric graben in the movable part. Experiments at lithospheric scale after *Beslier* [1991].

generates simultaneously the formation of two parallel and linear grabens separated by a horst: a half graben on the movable part and a near-symmetric graben on the motionless part (Figure 6b). At lithospheric scale, it is worth noting that the maximum value of thinning of the analogue crustal layers is located in the central part of the asymmetric graben, whereas the analogue layers of the mantle lithosphere are mostly thinned below the border of the horst. The difference observed between the geometry of the near-symmetric and asymmetric grabens in crustal and lithospheric experiments is likely to result from the uplift of the UBL due the activity of the detachment fault and the resulting isostatic adjustment in lithospheric experiments. Whatever the extension rate, the deformation of the UBL seems to be directly linked at lithospheric scale to the rupture of the LBL or at crustal scale to the velocity discontinuity. These results indicate that a low extension rate prevents the formation of the symmetric companion graben observed in high extension rate experiments.

[29] Using a vertically stratified silicone, the internal strain of the ductile layers has also been studied at lithospheric scale in high extension rate experiments [*Brun and Beslier*, 1996]. According to these authors, extension induces the formation of two conjugate shear zones in each ductile part of the models (i.e., the LDL and the UDL), which control the thinning of the whole lithospheric model (see Figure 5 of *Brun and Beslier* [1996]). They have proposed that the mode of lithospheric extension corresponds to a necking of the lithosphere that can lead to mantle exhumation just before oceanization [*Brun and Beslier*, 1996]. It is interesting to note that *Chemenda et al.* [2002] have also determined the occurrence of litho-

spheric shear zones controlling the thinning of the models. Nevertheless, their experiments show that for an evoluate stage of extension only one lithospheric shear zone prevails mimicking the simple shear mode proposed by *Wernicke* [1981, 1985] (see Figure 5 of *Chemenda et al.* [2002]). Such a result is in disagreement with the necking model

Figure 7. Internal strain of the silicone layers in high extension rate experiments deduced from the final geometry of the vertical markers in the silicone layers. Colors from light to dark blue indicate variations in strain intensity for the top-to-the-left shear zone whereas the yellow to red colors indicate strain intensity for the top-to-the-right shear zone (see text for explanation). See color version of this figure at back of this issue.
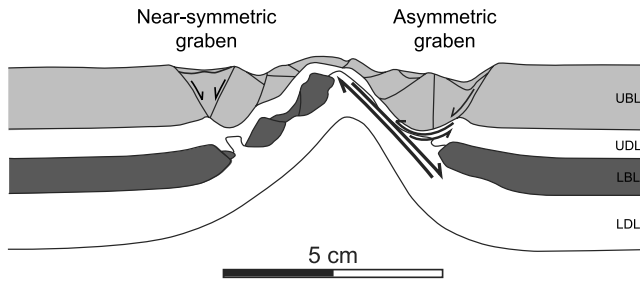
Figure 8. Cross section of an experiment at lithospheric scale characterized by a high extension rate and a nearly similar amount of extension (see text for explanation) (modified after *Brun and Beslier* [1996]).

proposed by *Brun and Beslier* [1996] where shear zone activity is coeval on both sides of the rift up to the formation of the ocean lithosphere.

3.3. New Results From the Comparison of Analogue Experiments at Crustal and Lithospheric Scale

[30] To solve the apparently different deformation at lithospheric scale, we compare the internal strain in the experiments at crustal and lithospheric scales.

[31] High extension rate experiments at crustal scale reveal that a VD always creates two conjugate shear zones in the ductile level, which are clearly related to the grabens in the UBL (see Figure 4 of *Michon and Merle* [2000]). Shear measurements also indicate that the top-to-the-left shear zone associated with the half graben always prevails with respect to the other one (Figure 7a). In contrast, the opposite shear zone, which is related to the near-symmetric graben is much less important and its activity decreases during extension.

[32] Using the same analytical approach in experiments at high extension rate, we have determined the internal strain of the silicone layers at lithospheric scale (Figure 7b). This clearly shows the occurrence of a continuous shear zone associated with the asymmetric graben which crosscuts the whole model down to the LDL. Such a shear zone is strikingly similar to the one observed in the experiments of *Chemenda et al.* [2002]. Very high shear strain is recorded in the UDL whereas strain is lower in the LDL. This major shear zone corresponds to a top-to-the-left low-angle detachment structure which controls the upwelling of the LBL. To this respect, it is interesting to note that the asymmetric shape of the glucose solution (i.e., the analogue asthenosphere) suggests that the detachment fault controls the thinning of the whole model. It is also possible to define two top-to-the-right shear zones that can be traced out in the UDL and the LDL (Figure 7a). Shear measurements deduced from the distortion of the initially vertical markers indicate that the highest shear strain along the shear zones are located below the asymmetric graben, that is in the UDL for the top-to the-left shear zone and in the LDL for the top-to-the-right shear zone. In a way similar to crustal scale experiments, the deformation concentrates along the major

detachment fault and the activity of the top-to-the-right shear zone in the UDL progressively decreases as it is suggested by the preservation of the initial geometry of the nearly symmetric graben.

[33] A second experiment at high extension rate (Figure 4a of *Brun and Beslier* [1996]) shows a different geometry at lithospheric scale. This model, conducted at an identical extension rate that the previous experiment (i.e., 5 cm/h), has been stopped at a slightly higher amount of extension (3.8 cm instead of 3.2 cm for the first experiment). The lack of vertically stratified silicone in the model does not allow the internal strain to be defined. Nevertheless, the geometry of the LBL with its uplift toward the nearly symmetric graben suggests that the deformation is controlled by the top-to-the-right shear zone located in the LDL (Figure 8). Crustal deformation is characterized by the development of a strongly asymmetric graben due to a top-to-the-left main shear zone in the UDL similar to the main shear zone observed in previous experiments. This top-to-the-left shear zone was passively deformed when the top-to-the-right shear zone became prominent (Figure 8). Thus, the total thinning of the model (i.e., mantle levels and crustal layers) is controlled by two conjugate and opposite main shear zones.

[34] In experiments at low extension rate, the internal strain of the silicone layers has not been studied in details. Nevertheless, the similar location and shape of the thinning of the silicone layer in crustal scale experiments also suggests the occurrence of two conjugate shear zones (Figure 9). We speculate that the top-to-the right shear zone in low rate experiments is not strong enough to induce the formation of a nearly symmetric graben in the UBL.

[35] All experiments suggest that a VD creates two opposite and conjugate shear zones in the ductile layers whatever the extension rate. This result is in agreement with purely brittle models in which a VD always leads to the
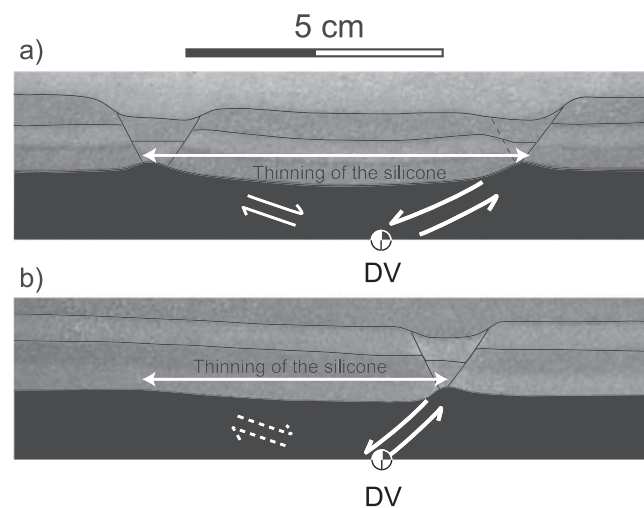
Figure 9. Comparison of the final geometry of the silicone layer in experiment at crustal scale with (a) high and (b) low extension rate. The similar shape of the thinning of the silicone layer suggests the occurrence of two conjugate shear zones in the experiments whatever the extension rate.
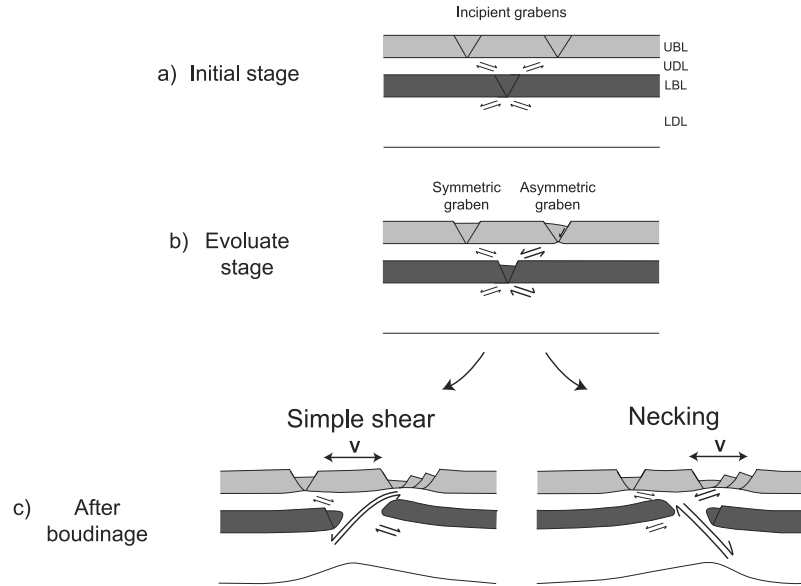
Figure 10. Synthetic evolution of the lithospheric deformation during continental rifting at high extension rates. During the initial stage of rifting, the extension induces (1) the development of conjugate shear zones in the ductile layers and (2) the formation of two incipient grabens. The evoluate stage is characterized by the predominance of two opposite shear zones located on the same vertical section. The crustal shear zone lead to the development of the asymmetric graben. When the brittle mantle lithosphere is broken out, the system can display two different mode of extension. In the necking model, the crustal shear zones control the crustal thinning and the mantle shear zone located below the asymmetric graben leads to the deformation of the mantle lithosphere. In the simple shear mode, the thinning and the deformation of the whole lithosphere is controlled by the shear zone associated with the asymmetric graben. V represents the potential location of the volcanism.

formation of two conjugate normal faults [e.g., *Faugère et al.*, 1986], and with the models of *Chemenda et al.* [2002] where the lithosphere is modeled by an elasto-plastic material. It also shows that the role of the top-to-the-right shear zone increases as a function of the extension rate.

[36] To sum up, analysis of the internal strain in the silicone layers shows (1) the development of two conjugate shear zones in each ductile level (i.e., the UDL and LDL) and (2) that the two shear zones located below the asymmetric graben predominate. Deformation of the mantle lithosphere levels in a final stage (i.e., after the boudinage of the LBL) is controlled by the shear zone located either in the UDL (Figure 7) or in the LDL (Figure 8).

4. Interpretation and Discussion

4.1. Modes of Lithospheric Extension During Continental Rifting

[37] Although analogue models at crustal and lithospheric scale have been carried out using different apparatus, the experimental results show striking similarities, proving that modeled deformation is indicative of a common tectonic process. As it has already been suggested [*Beslier*, 1991], we interpret the final geometry of crustal layers as resulting from the rupture of the brittle mantle.

[38] In high extension rate experiments, this rupture induces at the initial stage of extension a mirror symmetric deformation characterized by conjugate shear zones on both sides of the brittle mantle lithosphere (i.e., in the lower crust and the mantle ductile lithosphere) (Figure 10a). During this stage, the shear zones in the lower crust are responsible for the creation of two incipient grabens in the upper crust. This mode of extension mimics a pure shear deformation. With increasing amount of extension, this symmetric evolution stops. The activity of two shear zones is enhanced and they become prominent with respect to the two others. They are located on the same vertical section, one in the UDL and the other in the LDL (Figure 10b). The shear zone, which prevails in the UDL, induces the formation of an asymmetric graben (Figure 10b). In nature, this evolution is thought to originate the formation of an asymmetric graben (i.e. a half-graben) associated with a master normal fault in the upper brittle crust.

[39] Experiments at lithospheric scale show two different final geometries for a nearly similar amount of extension [*Brun and Beslier*, 1996]. These experiments reveal that during a later stage, the boudinage of the brittle mantle lithosphere leads to two contrasting evolutions resulting from the relative role of the main shear zones located in the lower crust and the ductile mantle lithosphere. If the UDL shear zone associated with the asymmetric graben prevails with respect to the mantle shear zone, boudinage of the brittle mantle lithosphere induces the formation of a master shear zone (i.e., a low-angle detachment structure), which crosscuts and controls the thinning of the whole lithosphere (Figure 10c left). In contrast, when the top-to-
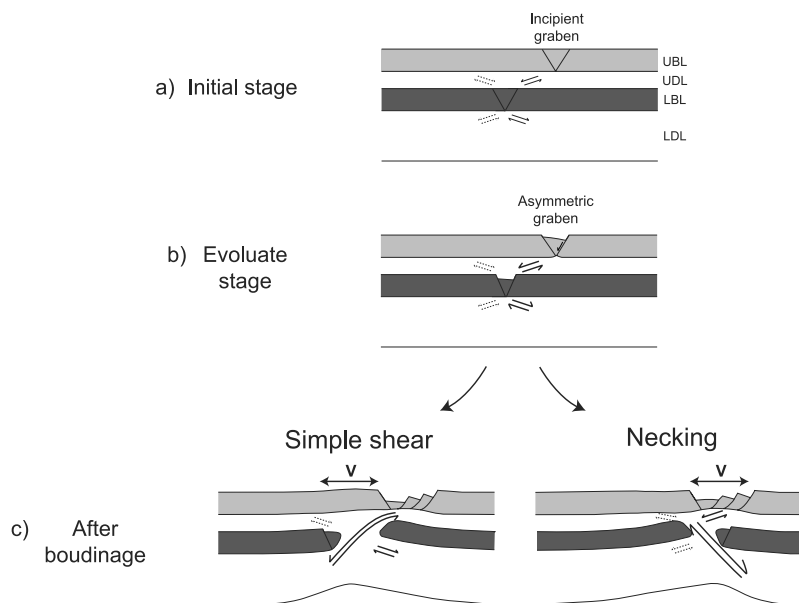
Figure 11. Synthetic evolution of the lithospheric deformation during continental rifting at low extension rates. During the initial stage of rifting, the extension induces (1) the development of conjugate shear zones in the ductile layers and (2) the formation of one incipient grabens. The evoluate stage is characterized by the predominance of two opposite shear zones located on the same vertical section. The crustal shear zone lead to the development of the asymmetric graben. When the brittle mantle lithosphere is broken out, the system can display two different mode of extension. In the necking model, the crustal shear zones control the crustal thinning and the mantle shear zone located below the asymmetric graben leads to the deformation of the mantle lithosphere. In the simple shear mode, the thinning and the deformation of the whole lithosphere is controlled by the shear zone associated with the asymmetric graben. V represents the potential location of the volcanism.

the-right shear zone located in the ductile mantle lithosphere is connected with the UDL shear zone associated with the nearly symmetric graben, the thinning of the lithosphere mainly results from the coeval activity of the two opposite and main shear zones (Figure 10c right). Thus, starting from a similar geometry before the boudinage of the brittle mantle lithosphere, extension can induce two different modes of extension: a simple shear mode which presents real similarities with the model proposed by *Wernicke* [1985], or a necking of the lithosphere as it has been described by *Brun and Beslier* [1996].

[40] In low extension rate experiments, it is assumed that during the initial stage, rupture of the brittle mantle lithosphere induces the formation of two conjugate shear zones in each ductile layer. However, experiments show that only one UDL shear zone is strong enough to initiate a graben in the upper crust. The resulting geometry defined by the set of shear zones corresponds to a mirror symmetry on both sides of the brittle mantle lithosphere (Figure 11a). As in the high extension rate evolution, subsequent deformation is controlled by the two main and opposite shear zones located in the ductile mantle lithosphere and the lower crust (Figure 11b). If the shear zone associated with the asymmetric graben prevails with respect to the mantle shear zone, a single low-angle detachment structure crosscuts the whole lithosphere when the brittle mantle lithosphere is broken out. The mode of extension then corresponds to a simple

shear mode and the maximum thinning of the crustal layers and the mantle lithospheric levels are not located on the same vertical line (Figure 11c left). If the shear zone of the ductile mantle lithosphere controls the deformation, the thinning of the different layers is vertically superposed, corresponding to the necking mode of extension (Figure 11c right).

[41] In experiments at lithospheric scale, the sand layer which represents the LBL is an isotope level without any previous fault and the difference of magnitude between the main shear zones can explain the different evolutions toward a simple shear or a necking mode. In nature, the previous history of a tectonic province can control the formation of structures at lithospheric scale. For example, an inherited structure in the brittle mantle lithosphere can be reactivated during continental extension and its geometry might favor the necking model or the simple shear mode.

[42] To sum up, the extension rate is a key parameter which controls the geometry of crustal deformation [*Michon and Merle*, 2000]. At low extension rate, extension induces the formation of a single asymmetric graben, whereas extension leads to the formation of two grabens at high extension rate. At lithospheric scale, deformation is mainly controlled by two opposite and main shear zones located below the asymmetric graben in the lower crust and the ductile mantle lithosphere. The thinning mode (i.e., simple shear or necking) is determined by the relative magnitude of

	Necking model	Simple shear mode
Low extension rate	*Eger graben*	*Red Sea rift* (Rhine graben)
High extension rate	*Massif Central Rift*	*North Atlantic passive margins*

Figure 12. Table showing the interpretation of the different provinces studied in this paper.

these two main shear zones, which may be due to the reactivation of inherited structures in the lithosphere. In both models, the thinning of the lithosphere may induce a volcanic activity by adiabatic decompression of the mantle. Volcanism should occur into the asymmetric graben with the necking mode and across the rift shoulder facing the master fault in the simple shear mode. These differences in the continental rift evolution can be considered as evidences which make possible to decipher the mode which has occurred in nature.

4.2. Application to Natural Examples

[43] In the first part of this paper, the review of the main geological features characterizing some continental rift has shown different evolutions which can exist in nature. We now apply our model to the natural laboratories in order to interpret their evolution.

4.2.1. Crustal Geometry

[44] At crustal scale, the Eger graben, the Red Sea rift and the Rhine graben correspond to single asymmetric grabens whereas major extensional structures created before oceanization in the North Atlantic passive margins (the Deep Galicia margin and the East Canadian margin) can be described as a pair of two companion grabens. We argue that these two types of basic structures result from a difference in the extension rate as already proposed by *Michon and Merle* [2000] for the Rhine graben and the Massif Central rift. This suggests that in the Eger graben and the Red Sea rift where the extension rate during the early stage of rifting is unknown, the extension rate was probably lower than in the North Atlantic passive margins (Figure 12). Using the relation between the strength ratio and the extension rate [*Michon and Merle*, 2000], an extension rate lower than 2 mm/yr can be proposed for the Eger graben and the first period of extension in the Red Sea rift. Likewise, an extension rate higher than 2 mm/yr may have induced the formation of the Deep Galicia margin and the Jeanne d'Arc basin.

[45] In the different areas (Eger graben, Red Sea rift and North Atlantic passive margins), the occurrence of one or two grabens also indicates that the crustal deformation was caused by a single rupture in the brittle mantle lithosphere. The Massif Central rift geometry could be explained by (1)

the occurrence of two simultaneous ruptures of the brittle mantle lithosphere initially spaced by around 50 km and (2) a high extension rate [*Michon and Merle*, 2000].

4.2.2. Mode of Extension

[46] In the Red Sea rift and the North Atlantic passive margins, geological data plead for a simple shear mode with the development of a main low-angle detachment structure. In the North Atlantic passive margins, such a mode of extension allows to explain (1) the predominance of the reflector S (the crustal shear zone) upon the mantle shear zone and (2) the lack of mantle lithospheric thinning below the Jeanne d'Arc basin as it has been shown by *Keen and Dehler* [1993]. Thus, the extension was mainly controlled by a single detachment structure connected with the Deep Galicia margin, which may have caused the exhumation of the lithospheric mantle before oceanization. In such a process, shifting of the extension from the Interior Basin toward the Deep Galicia margin suggests that the deformation narrows during lithospheric extension.

[47] Following *Wernicke* [1985], we consider that the asymmetric geological features resulting from the Late Oligocene-Early Miocene evolution in the Red Sea rift can be interpreted as the consequence of the activity of a single low-angle detachment structure. In contrast, the present-day data suggest that the mode of lithospheric extension which is interpreted as the result of a pure shear mode [*Buck et al.*, 1988] has changed. This indicates that the mode of extension during continental rifting probably evoluates toward a mode of extension where the pure shear deformation prevails during oceanization. At lithospheric scale, the nearly symmetric shape of opposite passive margins could therefore result from a change in the mode of extension after the onset of oceanization.

[48] Assuming that the magmatic activity appears above the zone of maximum lithospheric thinning, the occurrence of a syn-rift volcanic phase located within the graben areas in the Eger graben and the Massif Central rift cannot be explained by a simple shear mode for which the maximum of lithospheric thinning is located outside the graben. An alternative explanation is that the crust is affected by a single detachment structure, whereas the mantle lithosphere is thinned in pure shear mode (Figure 3d of *Lister et al.* [1991]). However, in this model, the mantle lithosphere is considered as purely ductile and the resulting strength profile does not correspond to the strength profile of a lithosphere with a normal thermal gradient [*Davy and Cobbold*, 1991]. In addition, experiments show that once the lithosphere is characterized by a brittle mantle layer, the rupture of this brittle part induces the development of shear zones in both the lower crust and the ductile mantle lithosphere. This is why we believe that the Eger graben and the Late Oligocene-Early Miocene evolution of the Massif Central rift result from lithospheric necking. In these provinces, necking of the lithosphere has induced a crustal thinning in the asymmetric graben and the development of a syn-rift volcanism into the graben. In the Eger graben, data at crustal scale suggest small stretching values, whereas the occurrence of the volcanic phase indicates a strong mantle lithospheric thinning. Such a paradox can be

explained by decoupling the crustal and mantle lithospheric deformations along the Moho mechanical discontinuity [*Fleitout*, 1984].

[49] Although the Rhine Graben likely results from a low extension rate [*Michon and Merle*, 2000], the mode of lithospheric extension cannot be surely constrained with available geological data as both lithospheric necking and simple shear mode can generate a single asymmetric graben. We can only speculate that the reflectors visible below the Moho and in the continuity of the major fault [*Brun et al.*, 1992] could represent a part of a continuous detachment-like structure, which crosscuts the whole lithosphere as in the simple shear mode.

[50] These conceptual models, based on analogue experiments, indicate that the extension rate and the mode of extension are the main parameters, which control the geometry of the continental rifts and passive margins. Recent numerical experiments suggest that rheological softening at lithospheric scale can also act on the symmetry of lithospheric extension, and has a complex interaction with the rate of extension [*Huismans and Beaumont*, 2002]. Also, even if our models can explain the main characteristics of several continental rifts, the role of the rheological distribution at lithospheric scale and sub-surface processes (i.e., erosion and syn-rift sedimentation) should be considered as potential parameters which can influence the geometry of deformation during continental rifting, as it has been proposed by *Burov and Cloetingh* [1997] and *Burov and Poliakov* [2001] for post-rift evolution.

5. Conclusions

[51] This study first shows that two independent sets of analogue experiments carried out at crustal [*Michon and Merle*, 2000] and lithospheric scale [*Beslier*, 1991; *Brun and Beslier*, 1996] can be compared if the models were initially properly scaled.

[52] As it has already been proposed [*Michon and Merle*, 2000], the extension rate plays a major role on the crustal deformation. Narrow rifts (single half-grabens) are formed with low extension rates whereas wider rift (two grabens) results from larger extension rate. According to *Michon and Merle* [2000], the development of more than two individual grabens (e.g., the Massif Central rift) results from several ruptures in the brittle mantle lithosphere.

[53] This study based on analogue experiments also shows an identical initial rifting stage characterized by two main shear zones, located below the asymmetric graben in the lower crust and the ductile mantle lithosphere. With increasing extension, these two main shear zones may produce a simple shear mode which shows similarities with the model proposed by *Wernicke* [1981, 1985], or a lithospheric necking as described by *Brun and Beslier* [1996]. These results allow an interpretation of the evolution of the Rhine graben, the Eger graben, the Massif Central rift, the Red Sea rift and the North Atlantic passive margins. In addition, these results could be applied to the North Sea rift where several mantle lithospheric shear zones have been identified by seismic studies [*Reston*, 1993].

[54] Finally, this study suggests an evolution of the mode of deformation during extension. The continental rifting is mainly characterized by a simple shear deformation that induces asymmetric structure in the crust. In contrast, pure shear deformation probably prevails during oceanization, explaining the global symmetry of conjugate passive margins superimposed to the asymmetry of the crustal deformation inherited from the continental rift stage.
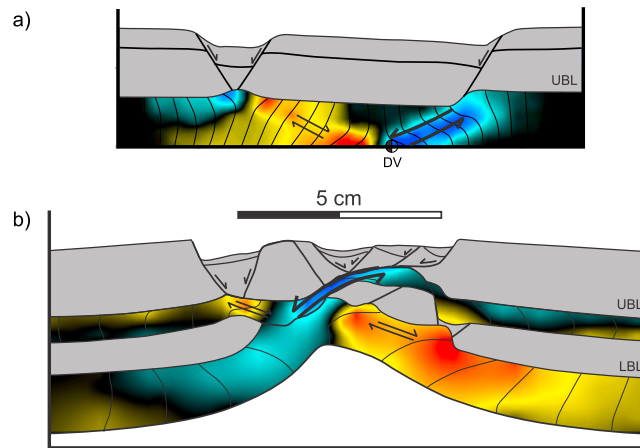
References

Allemand, P., J.-P. Brun, P. Davy, and J. Van Den Driessche, Symetrie et asymetrie des rifts et mecanismes d'amincissement de la lithosphere, *Bull. Soc. Geol. Fr.*, 5, 445–451, 1989.

Baker, J., L. Snee, and M. Menzies, A brief Oligocene period of flood volcanism in Yemen: Implications for the duration and rate of continental flood volcanism at the Afro-Arabian triple junction, *Earth Planet. Sci. Lett.*, 138, 39–55, 1996.

Beslier, M. O., Formation des marges passives et remontée du manteau: Modélisation expérimentale et exemple de la marge de la Galice, *Mém. Géosci. Rennes*, 45, 199 pp., 1991.

Beslier, M. O., J. Girardeau, and G. Boillot, Kinematics of peridotite emplacement during North Atlantic continental rifting, Galicia, northwestern Spain, *Tectonophysics*, 184, 321–343, 1990.

Bodergat, A. M., D. Briot, M. Hugueney, J. L. Poidevin, L. Picot, F. Giraud, J. P. Berger, A. Levy, and A. Poignant, Incursions marines dans l'environnement lacustre du rift oligocène de Limagne (Massif central, France): Apport des organismes halophiles et des isotopes du strontium; datation par les mammifères, *Bull. Soc. Géol. Fr.*, 170, 499–511, 1999.

Bohannon, R. G., C. W. Naeser, D. L. Schmidt, and A. Zimmermann, The timing of uplift, volcanism, and rifting peripheral to the Red Sea: A case for passive rifting?, *J. Geophys. Res.*, 94, 1683–1701, 1989.

Boillot, G., S. Grimaud, A. Mauffret, D. Mougenot, J. Kornprobst, J. Mergoil-Daniel, and G. Torrent, Ocean-continent boundary off the Iberian margin: A serpentinite diapir west of the Galicia bank, *Earth Planet. Sci. Lett.*, 48, 23–34, 1980.

Boillot, G., et al., *Proceedings of the Ocean Drilling Program: Scientific Results*, vol. 103, 858 pp., Ocean Drill. Program, College Station, Tex., 1988.

Boillot, G., M. O. Beslier, C. M. Krawczyk, D. Rappin, and T. J. Reston, The formation of passive margins: Constraints from the crustal structure and segmentation of the deep Galicia margin (Spain), in *The Tectonic, Sedimentation and Palaeoceanography of the North Atlantic Region*, edited by M. S. Stocker, G. B. Shimmlied, and A. W. Tudhope, *Geol. Soc. Spec. Publ.*, 90, 71–91, 1995.

Bois, C., Initiation and evolution of the Oligo-Miocene rift basins of southwestern Europe: Contribution of deep seismic reflection profiling, *Tectonophysics*, 226, 227–252, 1993.

Bosworth, W., Geometry of propagating continental rifts, *Nature*, 316, 625–627, 1985.

Brown, G. F., D. L. Schmidt, and A. C. Huffman, Geology of the Arabian Peninsula shield area of western Saudi Arabia, *U.S. Geol. Surv. Open File Rep.*, OF-84-0203, 217 pp., 1984.

Brun, J. P., Narrow rifts versus wide rifts: Inferences for the mechanics of rifting from laboratory experiments, *Philos. Trans. R. Soc. London, Ser. A*, 357, 695–712, 1999.

Brun, J. P., and M. O. Beslier, Mantle exhumation at passive margin, *Earth Planet. Sci. Lett.*, 142, 161–173, 1996.

Brun, J. P., M. A. Gutscher, and DEKORP-ECORS Teams, Deep crustal structure of the Rhine Graben from DEKORP-ECORS seismic reflexion data: A summary, *Tectonophysics*, 208, 139–147, 1992.

Buck, W. R., Modes of continental lithospheric extension, *J. Geophys. Res.*, 96, 20,161–20,178, 1991.

Buck, W. R., F. Martinez, M. S. Steckler, and J. R. Cochran, Thermal consequences of lithospheric extension: Pure and simple, *Tectonics*, 7, 213–234, 1988.

Burov, E., and S. Cloetingh, Erosion and rift dynamics: New thermomechanical aspects of post-rift evolution of extensional basins, *Earth Planet. Sci. Lett.*, *150*, 7–26, 1997.

Burov, E., and A. Poliakov, Erosion and rheology controls on synrift and postrift evolution: Verifying old and new ideas using a fully coupled numerical model, *J. Geophys. Res.*, *106*, 16,461–16,481, 2001.

Chazot, G., M. A. Menzies, and J. Baker, Pre-, syn- and post-rift volcanism on the south-western margin of the Arabian plate, in *Sedimentation and Tectonics of rift Basins*: *Red-Sea-Gulf of Aden*, edited by B. H. Purser and D. W. J. Bosence, pp. 50–55, Chapman and Hall, New York, 1998.

Chemenda, A., J. Deverchere, and E. Calais, Three-dimensional laboratory modelling of rifting: Application to the Baikal rift, Russia, *Tectonophysics*, *356*, 253–273, 2002.

Chlupac, I., O. Kodym, M. Suk, V. Holub, M. Elias, I. Cicha, M. Malkovsky, J. Tyracek, E. Mencyk, and T. Buday, Stratigraphic development of the units, in *Geological History of the Territory of the Czech Socialist Republic*, edited by M. Suk et al., pp. 87–200, Geol. Surv., Prague, 1984.

Cochran, J. R., and F. Martinez, Evidence from the northern Red Sea on the transition from continental to oceanic rifting, *Tectonophysics*, *153*, 25–53, 1988.

Courtillot, V. E., Opening of the Gulf of Aden and Afar by progressive tearing, *Phys. Earth Planet. Inter.*, *21*, 343–350, 1980.

Davy, P., and P. R. Cobbold, Experiments on shortening of a 4-layer model of the continental lithosphere, *Tectonophysics*, *188*, 1–25, 1991.

Dixon, T. H., E. R. Ivins, and B. J. Franhlin, Topographic and volcanic asymmetry around the Red Sea: Constraints on rift models, *Tectonics*, *8*, 1193–1216, 1989.

Doebl, F., and W. Olbrecht, An isobath map of the Tertiary base in the Rhine graben, in *Approaches to Taphrogenesis*: *Proceedings of an International rift Symposium Held in Karlsruhe*, edited by J. H. Illies and K. Fuchs, pp. 71–72, Schweizerbart, Stuttgart, Germany, 1974.

Driscoll, N. W., J. R. Hogg, N. Cristie-Blick, and G. Karner, Extensional tectonics in the Jeanne d'Arc Basin, offshore Newfoundland: Implications for the timing of the break-up between Grand Banks and Iberia, in *The Tectonic, Sedimentation and Palaeoceanography of the North Atlantic Region*, edited by M. S. Stocker, G. B. Shimmlied, and A. W. Tudhope, *Geol. Soc. Spec. Publ.*, *90*, 1–28, 1995.

Faugère, E., J. P. Brun, and J. van dan Driessche, Bassins asymétriques en extension pure et en décrochement: Modèles expérimentaux, *Bull. Cent. Rech. Explor. Prod. Elf Aquitaine*, *10*, 13–21, 1986.

Féraud, G., J. Girardeau, M. O. Beslier, and G. Boillot, Datation ^{39}Ar/^{40}Ar de la mise en place des peridotites bordant la marge de la Galice (Espagne), *C. R. Acad. Sci. Paris*, *307*, 49–55, 1988.

Fernandez, M., and G. Ranalli, The role of rheology in extensional basin formation modeling, *Tectonophysics*, *282*, 129–145, 1997.

Fleitout, L., Modélisation des contraintes tectoniques et des instabilités thermo-mécaniques dans la lithosphère, Thèse d'état, 433 pp., Univ. Orsay, France, 1984.

Girardeau, J., C. A. Evans, and M. O. Beslier, Structural analysis of plagioclase-bearing peridotites emplaced at the end of continental rifting: Hole 637A, ODP Leg 103 on Galicia margin, *Proc. Ocean Drill. Program Sci. Results*, *103*, 209–223, 1988.

Giraud, J., Etudes géologiques sur la Limagne (Auvergne), Thèse d'état, 410 pp., Ed. Ch. Béranger, Paris, 1902.

Granet, M., S. Judenherc, and A. Souriau, Des images du système lithosphère-asthénosphère sous la France et leurs implications géodynamiques: L'apport de la tomographie télésismique et de l'anisotropie sismique, *Bull. Soc. Géol. Fr.*, *171*, 149–167, 2000.

Hubbert, K. M., Theory of scale models as applied to the study of geologic structures, *Geol. Soc. Am. Bull.*, *48*, 1459–1520, 1937.

Huismans, R. S., and C. Beaumont, Asymmetric lithospheric extension: The role of frictional plastic strain softening inferred from numerical experiments, *Geology*, *30*, 211–214, 2002.

Jaeger, J. C., and N. G. W. Cook, *Fundamental of Rock Mechanics*, 585 pp., Chapman and Hall, New York, 1971.

Keen, C. E., and S. A. Dehler, Stretching and subsidence: rifting of conjugate margins in the North Atlantic Region, *Tectonics*, *12*, 1209–1229, 1993.

Kooi, H., M. Hettema, and S. Cloetingh, Lithospheric dynamics and the rapid Pliocene-Quaternary subsidence phase in the Southern North Sea Basin, *Tectonophysics*, *192*, 245–259, 1991.

Kusznir, N. J., and P. A. Ziegler, The mechanics of continental extension and sedimentary basin formation: A simple-shear/pure-shear flexural cantilever model, *Tectonophysics*, *215*, 117–131, 1992.

Le Pichon, X., and J. M. Gaulier, The rotation of Arabia and the Levant Fault System, *Tectonophysics*, *153*, 271–294, 1988.

Lister, G. S., M. A. Etheridge, and P. A. Symonds, Detachment models for the formation of passive continental margins, *Tectonics*, *10*, 1038–1064, 1991.

Manatschal, G., and D. Bernoulli, Architecture and tectonics evolution of nonvolcanic margins: Present-day Galicia and ancient Adria, *Tectonics*, *18*, 1099–1119, 1999.

Mart, Y., and J. K. Hall, Structural trends in the northern Red Sea, *J. Geophys. Res.*, *89*, 11,352–11,354, 1984.

Mauffret, A., and L. Montadert, Rift tectonics on the passive continental margins off Galicia (Spain), *Mar. Pet. Geol.*, *4*, 49–70, 1987.

McKenzie, D., Some remarks on the development of sedimentary basins, *Earth Planet. Sci. Lett.*, *40*, 25–42, 1978.

Menzies, M., J. Baker, G. Chazot, and M. Al'Kadasi, Evolution of the Red sea volcanic margin, Western Yemen: Large igneous provinces, in *Continental, Oceanic, and Planetary Flood Volcanism*, *Geophys. Monogr. Ser.*, vol. 100, edited by J. Mahoney and M. Coffin, pp. 29–43, AGU, Washington, D. C., 1997.

Merle, O., and A. Borgia, Scaled experiments of volcanic spreading, *J. Geophys. Res.*, *101*, 13,805–13,817, 1996.

Merle, O., L. Michon, and G. Camus, L'extension oligocène sur la transversale septentrionale du rift du Massif Central, *Bull. Soc. Géol. Fr.*, *169*, 615–626, 1998.

Merle, O., N. Vidal, and B. Van Wyk de Vries, Experiments on vertical basement fault reactivation below volcanoes, *J. Geophys. Res.*, *106*, 2153–2162, 2001.

Michon, L., Dynamique de l'extension continentale-Application au rift Ouest-Européen par l'étude de la province du Massif Central, *Mém. Géosci. Rennes*, *99*, 266 pp., 2001.

Michon, L., and O. Merle, Crustal structures of the Rhinegraben and the Massif Central grabens: An experimental approach, *Tectonics*, *19*, 896–904, 2000.

Ranalli, G., and D. C. Murphy, Rheological stratification of the lithosphere, *Tectonophysics*, *132*, 281–296, 1987.

Rat, P., Le système Bougogne-Morvan-Bresse (articulation entre le bassin parisien et le domaine périalpin), in *Géologie de la France*: *Les Chaínes Plissées du Cycle Alpin et Leur Avant-Pays*, edited by J. Debelmas, pp. 480–500, Doin, Paris, 1974.

Reston, T. J., Evidence for extensional shear zones in the mantle, offshore Britain, and their implications for the extension of the continental lithosphere, *Tectonics*, *12*, 492–506, 1993.

Reston, J. T., C. M. Krawczyk, and D. Klaeschen, The S reflector west of Galicia (Spain): Evidence from prestack depth migration for detachment faulting during continental breakup, *J. Geophys. Res.*, *101*, 8075–8091, 1996.

Rittmann, U., and H. J. Lippolt, Evidence for distortion of Tertiary K/Ar ages by excess argon-example given by three alkali olivine basalts from Northern Hesse, Germany, *Eur. J. Mineral.*, *10*, 95–110, 1998.

Rosendahl, B. R., E. Kilembe, and K. Kaczmarick, Comparison of Tanganyika, Malawi, Rukwa and Turkana rift zones from analyses of seismic reflection data, *Tectonophysics*, *213*, 235–256, 1992.

Schumacher, M., Upper Rhine Graben: Role of preexisting structures during rift evolution, *Tectonics*, *21*(1), 1006, doi:10.1029/2001TC900022, 2002.

Sissingh, W., Comparative Tertiary stratigraphy of the Rhine Graben, Bresse Graben and Molasse Basin: Correlation of Alpine foreland events, *Tectonophysics*, *300*, 249–284, 1998.

Tankard, A. J., and H. J. Welsink, Extensional tectonics and stratigraphy of Hiberia Oil Field, Grand Banks, Newfoundland, *AAPG Bull.*, *71*, 1210–1232, 1987.

Ulrych, J., V. Cajz, E. Pivec, J. K. Novak, C. Nekovarik, and K. Balogh, Cenozoic intraplate alkaline volcanism of western Bohemia, *Stud. Geoph. Geod.*, *44*, 346–351, 2000.

Villemin, T., F. Alvarez, and J. Angelier, The Rhinegraben: Extension subsidence and shoulder uplift, *Tectonophysics*, *128*, 47–59, 1986.

Vissers, R. L. M., M. R. Drury, E. H. Hogerduijn Strating, C. J. Spiers, and D. van der Wal, Mantle shear zones and their effect on lithosphere strength during continental breakup, *Tectonophysics*, *249*, 155–171, 1995.

Wernicke, B., Low-angle normal faults in the Basin and Range Province: Nappe tectonics in an extending orogen, *Nature*, *291*, 645–648, 1981.

Wernicke, B., Uniform-sense normal simple shear of the continental lithosphere, *Can. J. Earth Sci.*, *22*, 108–125, 1985.

Zijerveld, L., R. Stephenson, S. Cloetingh, E. Duin, and M. W. van den Berg, Subsidence analysis and modelling of the Roer Valley Graben (SE Netherland), *Tectonophysics*, *208*, 159–171, 1992.

—————————

O. Merle, Laboratoire Magmas et Volcans, OPGC, Université Blaise Pascal, CNRS, F-63038 Clermont-Ferrand cedex, France.

L. Michon, Netherlands Organization for Applied Scientific Research–Netherlands Institute of Applied Geoscience (TNO-NITG), P.O. Box 80015, NL-3508 TA Utrecht, Netherlands. (l.michon@nitg.tno.nl)

Figure 7. Internal strain of the silicone layers in high extension rate experiments deduced from the final geometry of the vertical markers in the silicone layers. Colors from light to dark blue indicate variations in strain intensity for the top-to-the-left shear zone whereas the yellow to red colors indicate strain intensity for the top-to-the-right shear zone (see text for explanation).